

Millimeter-wave Passive Patch Antenna for Use in Wireless High-temperature Sensor

Ying-Ting Liao,¹ Yih-Chien Chen,^{2*} and Cheng-Chien Kuo¹

¹Department of Electrical Engineering, National Taiwan University of Science and Technology,
No. 43, Keelung Rd., Sec. 4, Da'an Dist., Taipei City 106335, Taiwan (R.O.C.)

²Department of Electrical Engineering, Lunghwa University of Science and Technology,
No. 300, Sec. 1, Wanshou Rd., Guishan District, Taoyuan City 333326, Taiwan (R.O.C.)

(Received December 30, 2021; accepted April 20, 2022)

Keywords: millimeter wave, wireless sensor, passive antenna temperature sensor

We propose a passive patch antenna temperature sensor architecture consisting of a transceiver and a passive patch antenna temperature sensor made of RO3003 and Mg₂SnO₄ ceramic substrates, respectively. The millimeter dielectric properties of Mg₂SnO₄ ceramic were examined with a view to its use as a wireless high-temperature passive patch antenna temperature sensor. A dielectric constant of 3.97 and a loss factor of 5.42×10^{-2} were obtained for Mg₂SnO₄ ceramic sintered at 1550 °C for 4 h. We report the development procedures and test results for a passive patch antenna temperature sensor. The resonating frequency and 3 dB bandwidth of the sensor measured at 25 °C were 30.6210 GHz and 1530 MHz, respectively. The measurement resonant frequency decreased from 30.6210 to 30.3790 GHz when the operating temperature increased from 25 to 225 °C, which correspond to a sensitivity and linearity of -1.210 MHz/°C and 0.06%, respectively.

1. Introduction

The increasing demand for energy in recent years has promoted the development of smart grids in many countries. A smart grid must collect and analyze a large amount of information in power networks and then make appropriate decisions and actions according to analysis results to improve the efficiency of the grid.⁽¹⁾ Many switchgear boards used in power networks are connected to the user end by high-voltage cables to distribute power. However, any device can fail, including the switchboard. A failure caused by connectors is most common.⁽²⁾ Taking the no fuse breaker (NFB) as an example, when a failure occurs at the connection, the temperature rises, accelerating the deterioration of the insulation material. When the structure of the insulation material is damaged, or the amount of insulation is reduced, the insulation ability between the two electrodes becomes unsatisfactory and high-temperature arcs are generated, leading to accidents. The influence of connection faults on temperature can be monitored through temperature sensors, and faults can be detected to avoid accidents. Owing to the extensive use of switchboards in power networks, there is a huge demand for the use of temperature sensors.

*Corresponding author: e-mail: ee049@mail.lhu.edu.tw
<https://doi.org/10.18494/SAM3841>

Sensors are divided into contact and remote sensing types.^(3,4) Contact sensors such as thermocouple temperature sensors are usually set on the measurement object and must be connected with the measurement instrument using cables.⁽⁵⁾ A remote sensor is a wireless temperature sensor, which has a low cost and is easy to set up, making it suitable for a wide range of applications.⁽⁶⁾ A remote sensor separates the measurement instrument from the sensor, eliminating the need for cables to connect them. In this study, the sensor is a passive component set on the measured object, a sensor wirelessly receives signals from a transceiver, to determine the object's temperature. Both the sensor and the transceiver are patch antennas.

Wireless temperature sensors are classified into two categories: electronic chip temperature sensors and chipless ones. The latter do not require the battery to be monitored or replaced regularly. The operating temperature of a chipless sensor is higher than that of an electronic chip sensor. Chipless sensors, such as chipless RFID tags,⁽⁷⁾ temperature sensors,⁽⁸⁾ and material strain sensors, were previously studied.^(9,10) Many types of passive wireless sensors have been developed. A surface acoustic wave (SAW) sensor is used to sense parameters such as pressure, torque, acceleration, humidity, magnetic field, soil moisture, gas, and temperature with high sensitivity.^(11,12) However, its chemical stability is low and its signal is susceptible to interference. An LC resonator sensor is easy to process and can be used in harsh environments. However, it cannot be used on a metal surface because high temperatures may significantly decrease the quality factor of the inductor.⁽¹³⁾ A temperature sensor equipped with a slot antenna and a micro-electromechanical (MEMS) system has been proposed.⁽¹⁴⁾ Although its measurable temperature can reach 300 °C, it is not suitable for metal surfaces. A dielectric resonator employing $Zr_{0.8}Sn_{0.2}TiO_4$ (ZST) has been used to study a wireless temperature sensor. Although the measurable temperature was up to 700 °C, the size of the dielectric resonator was large.⁽¹⁵⁾ Moreover, the emission efficiency of the dielectric resonator was negatively affected by its large dielectric constant. A microstrip patch antenna temperature sensor based on a commercial material can withstand a maximum temperature of 280 °C, although robustness at higher temperatures is still required.^(16–18) The concept and model of a metamaterial-based passive wireless temperature sensor suitable for applications in harsh environments have been reported, but no measurement experiments were performed.⁽¹⁹⁾

Sanders *et al.*⁽⁶⁾ reported a patch antenna temperature sensor made of an RO3006 substrate with a dielectric constant of 6.5 and a resonant frequency temperature coefficient of 63 ppm/°C. The resonant frequency of the sensing antenna was 5.862 GHz. The radiator was a patch antenna with a size of $11.8 \times 9.8 \text{ mm}^2$. The sensitivity of the sensing antenna was 0.703 MHz/°C. Chen and Du⁽²⁰⁾ reported a passive patch antenna temperature sensor made of a $(Mg_{0.93}Zn_{0.07})_2SnO_4$ ceramic substrate with a dielectric constant of 8.3 and a resonant frequency temperature coefficient of -69 ppm/°C. The resonant frequency of the sensing antenna was 2.48 GHz. The radiator was a passive patch antenna with a size of $28.1 \times 20.5 \text{ mm}^2$. The sensitivity of the sensing antenna was -0.169 MHz/°C. A comparison of the above antennas reported in Refs. 6 and 20 reveals that the higher the resonant frequency, the smaller the radiator size, and the resonant frequency must be increased to reduce the component size. A similar comparison indicates that the higher the resonant frequency, the greater the sensitivity. It is therefore necessary to increase the resonant frequency to increase the sensitivity. Moreover, $H=ms\Delta T$ can

be derived by converting the formula for the specific heat capacity, where H is the heat energy, m is the mass, and ΔT is the temperature change. According to this formula, the energy required to heat a sensor to a specific temperature is proportional to its mass, which in turn is proportional to its volume. Therefore, the sensor size can be reduced by increasing the resonant frequency, thus reducing the energy required for heating and the response time.

The general chemical formula of anti-spinel microwave ceramic materials is A_2BO_4 ($A = \text{Mg}^{2+}, \text{Zn}^{2+}, \text{Ni}^{2+}, \text{Co}^{2+}$; $B = \text{Sn}^{4+}, \text{Ti}^{4+}, \text{Zr}^{4+}$), where Zn_2TiO_4 has a dielectric constant of $\epsilon_r = 21$, a quality factor of $Q \times f = 20000$ GHz, and a resonant frequency temperature coefficient of $\tau_f = -60$ ppm/ $^\circ\text{C}$.⁽²¹⁾ The microwave dielectric properties of Zn_2SnO_4 include a dielectric constant of $\epsilon_r = 10.2$, a quality factor of $Q \times f = 39000$ GHz, and a resonant frequency temperature coefficient of $\tau_f = -84$ ppm/ $^\circ\text{C}$.⁽²²⁾ The microwave dielectric properties of Mg_2SnO_4 include a dielectric constant of $\epsilon_r = 8.4$, a quality factor of $Q \times f = 55100$ GHz, and a resonant frequency temperature coefficient of $\tau_f = -62$ ppm/ $^\circ\text{C}$.⁽²³⁾ Mg_2SnO_4 has the highest quality factor among these three materials, reducing the energy loss when it is used as an antenna substrate. It has been reported that the quality factor can be improved by replacing MgO with $4\text{MgCO}_3 \cdot \text{Mg}(\text{OH})_2 \cdot 4\text{H}_2\text{O}$ as the initial material, resulting in a dielectric constant of $\epsilon_r = 8.2$, a quality factor of $Q \times f = 59000$ GHz, and a resonant frequency temperature coefficient of $\tau_f = -64$ ppm/ $^\circ\text{C}$.⁽²⁴⁾ To our knowledge, the dielectric properties of Mg_2SnO_4 ceramics in millimeter waves have not been reported.

In this paper, we propose a wireless passive patch antenna temperature sensor architecture comprising a passive patch antenna with a custom-made ceramic substrate. The sensor is small and has high chemical stability, making it suitable for metal surfaces. RO3003 and Mg_2SnO_4 custom-made ceramic substrates were used for the transceiver and sensor antenna, respectively, to realize the passive patch antenna temperature sensor. The resonant frequency was designed to be at the millimeter-wave level to increase the sensitivity of the sensor; reduce its size, response time, and maintenance cost; avoid the use of batteries; and prevent short circuits between contacts.

2. Experimental Method

The conventional solid-state method was used to prepare the Mg_2SnO_4 ceramic substrate.^(21–24) The initial powder materials used to produce the Mg_2SnO_4 were $4\text{MgCO}_3 \cdot \text{Mg}(\text{OH})_2 \cdot 4\text{H}_2\text{O}$ (43.5%) and SnO_2 (99.9%), supplied by Alfa Aesar and Strem Chemicals, respectively. The required amount of each compound was obtained using an electronic scale. The Mg_2SnO_4 was calcinated at a heating rate of 10 $^\circ\text{C}/\text{min}$, a calcination temperature of 1200 $^\circ\text{C}$, and a temperature holding time of 4 h. Finally, the powder was pressed into pellets of 63 mm diameter and 3 mm thickness using a stainless steel mold and a uniaxial bidirectional molding press machine at a pressure of 2000 kg/cm². Dry pressurized molding was used in this study. The furnace temperature was increased from 650 to 1550 $^\circ\text{C}$ at a rate of 10 $^\circ\text{C}/\text{min}$, then held at 1550 $^\circ\text{C}$ for 4 h to sinter the specimen. The microwave dielectric properties of the specimen were measured using the post-resonator method developed by Hakki and Coleman.⁽²⁵⁾ The dielectric constant and quality factor were calculated from the resonant frequency and the measured dimensions of the sample.

The method for measuring the dielectric properties depicted above is not suitable for characterizing the Mg_2SnO_4 ceramic substrate in the millimeter range. Instead, the dielectric properties were measured by the Delta-L methodology.⁽²⁶⁾ This methodology employs two 50 ohm coplanar waveguide–micro stripline–coplanar waveguide configurations to measure the dielectric properties in the millimeter range, as shown in Fig. 1. One micro stripline must be longer than the other to obtain accurate results. Two G-S-G probes are connected to the coplanar waveguides of the specimen to transmit the signal power in or out of the micro stripline. The other end of each G-S-G probe is connected to a Keysight N5224A microwave network analyzer, which is used to measure the scattering parameters of the specimen, and the dielectric constant and the loss tangent are calculated.

An LPKF ProtoLaser U4 laser (LPKF Laser & Electronics, Germany) was used to fabricate the passive patch antenna temperature sensor with the Mg_2SnO_4 ceramic substrate and the transceiver with the RO3003 substrate (Rogers Corporation, US). The Mg_2SnO_4 ceramic substrate was ground to the required thickness with a grinding machine. The surface was polished with a polishing cloth and polishing fluid. Then, it was immersed in acetone and vibrated for 20 min with an ultrasonic vibrator to remove surface impurities. After vibration, the substrate was washed with deionized water for 20 min, then it was dried in a hot air circulation oven. Finally, silver glue was coated on the upper and lower surfaces of the substrate, and the substrate was dried in a hot air circulation oven at 150 °C for 1 h to make the silver glue completely adhere to its surface.

Figure 2 shows the architecture of the passive patch antenna temperature sensor, which used the orthogonal polarization method to measure signals. Short-Open-Load-Through calibration was performed before the experiment, and a Keysight Calibration Kit was used to eliminate errors due to source/load mismatch or isolation. A Keysight N5224A network analyzer was used to measure the resonant frequency of the passive patch antenna temperature sensor. Because the sensor adopted a passive design, the transceiver antenna was connected to the vector network analyzer through the coaxial cable and used as a transmitter and a reader. The transceiver

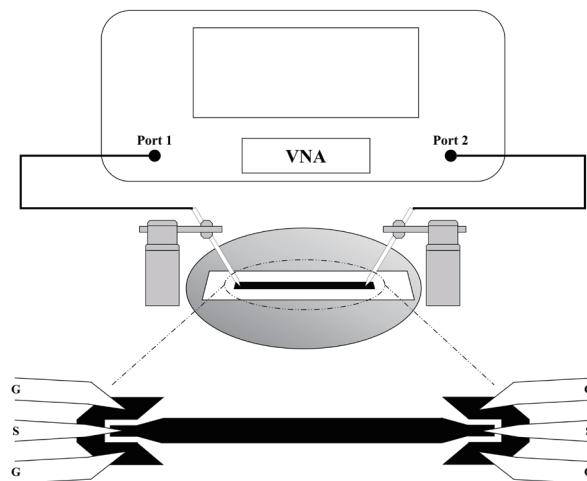


Fig. 1. Configuration used in measurement of millimeter dielectric properties.

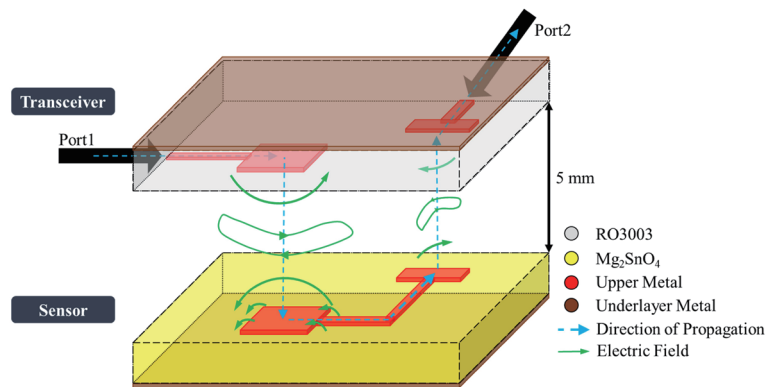


Fig. 2. (Color online) Architecture of passive patch antenna temperature sensor.

antenna was placed above the passive patch antenna temperature sensor. The two orthogonal patch antennas were connected to form a sensing antenna, which was placed in the heater. The transceiver antenna sends signals to the sensing antenna and receives backscattering signals, so as to realize the passive patch antenna temperature sensor. The sensitivity and linearity characteristics of the temperature sensor were analyzed.

3. Results and Discussion

Figure 3 shows the dielectric constant and loss factor of the Mg_2SnO_4 ceramic in the frequency range of 16–30 GHz at room temperature (25 °C). The dielectric constants in the range from 28 to 31 GHz were smaller than that around 16 GHz.⁽²⁴⁾ This can be explained by the dielectric polarization. The dielectric properties in the frequency range of 10–30 GHz were determined by ionic polarization. The Clausius-Mossotti formula is applicable to microscopic quantities and relations associated with polarization:⁽²⁷⁾

$$\varepsilon_r = \frac{3M + 8\pi N_A \alpha_D \rho}{3M - 4\pi N_A \alpha_D \rho}, \quad (1)$$

where ε_r , M , ρ , N_A , and α_D are the relative permittivity, molecular weight, density, Avogadro constant, and ionic dielectric polarization, respectively. This formula indicates that the larger the ionic dielectric polarization, the larger the dielectric constant will be. A higher frequency is well known to be associated with a lower ionic dielectric polarization.⁽²⁸⁾ Therefore, the dielectric constants in the range from 28 to 30 GHz were smaller than that at 16 GHz. Moreover, the loss factors in the range from 28 to 31 GHz were larger than that at 16 GHz. This was because the product of the quality factor and the resonant frequency is a constant for microwave ceramics. Therefore, as the frequency increased, the quality factor decreased and the loss factor increased.

Figure 4 shows the structure of the transceiver antenna with the RO3003 substrate. The dielectric constant of the substrate was 2.87, the loss tangent was 1.67×10^{-2} , and the thicknesses

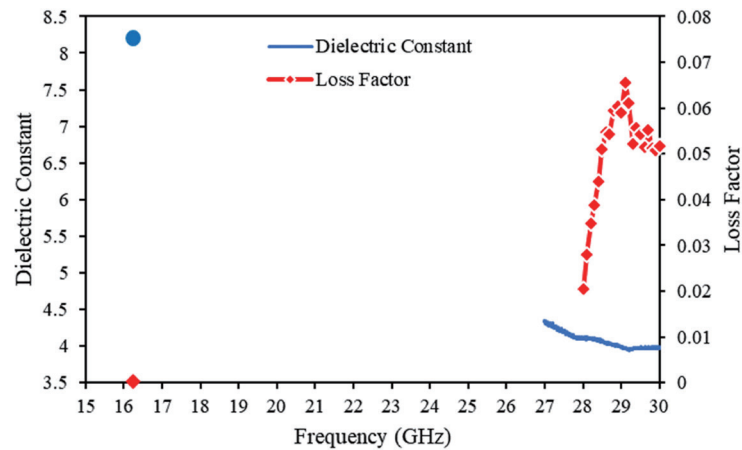


Fig. 3. (Color online) Dielectric constant and loss factor of Mg_2SnO_4 ceramic in the range of 16–30 GHz.

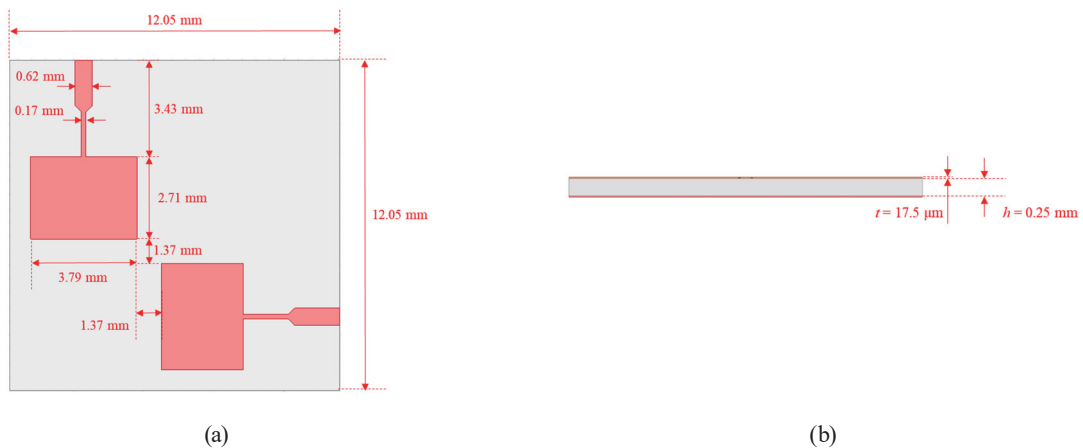


Fig. 4. (Color online) (a) Top view and (b) side view of structure of transceiver antenna with RO3003 substrate.

of the substrate and copper foil were 0.25 mm and 17.5 μm , respectively. Figure 5 shows the simulation and measurement results of the return loss of the transceiver antenna on the RO3003 substrate. The two sets of results were in good agreement. The resonant frequency, bandwidth, and return loss obtained by simulation were 30.015 GHz, 1678 MHz, and 27.42 dB, respectively. The measured resonant frequency, bandwidth, and return loss were 30.011 GHz, 1993 MHz, and 16.05 dB, respectively. Figure 6 shows the simulation and measurement results of the isolation degree of the transceiver antenna with the RO3003 substrate. The measured isolation degree was less than -20 dB from 28.00 to 32.00 GHz, indicating that the transceiver antenna exhibited good isolation between the transmitting and receiving antennas.

Figure 7 shows the structure of the passive patch antenna temperature sensor with the Mg_2SnO_4 substrate. The dielectric constant and loss tangent of the substrate were 3.97 and 5.42×10^{-2} , respectively. The substrate thickness and metal thickness were 0.5 mm and 40 μm , respectively. Figure 8 shows the simulation and measurement results of the return loss of the passive patch antenna temperature sensor on the Mg_2SnO_4 substrate. The resonant frequency,

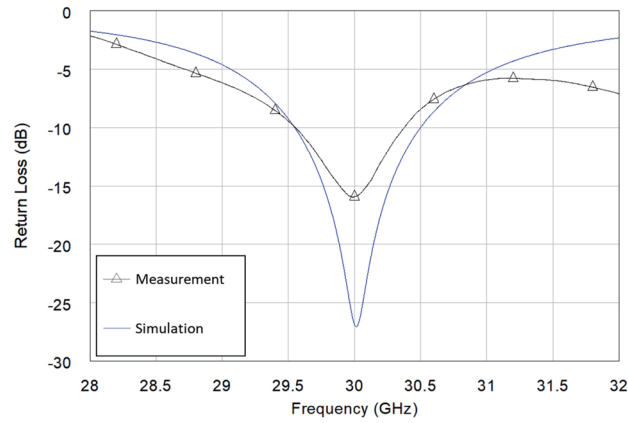


Fig. 5. (Color online) Simulation and measurement results of return loss of transceiver antenna on RO3003 substrate.

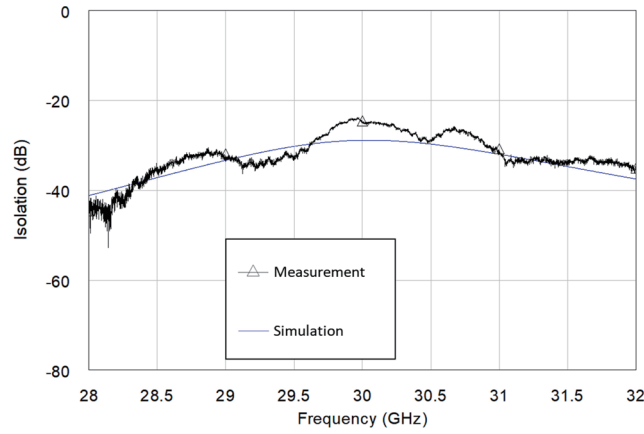


Fig. 6. (Color online) Simulation and measurement results of isolation degree of transceiver antenna on RO3003 substrate.

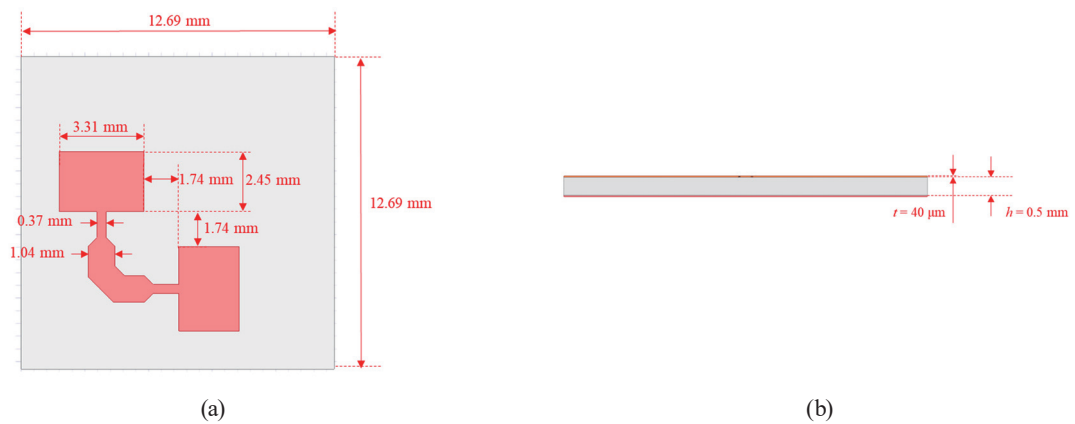


Fig. 7. (Color online) (a) Top view and (b) side view of structure of sensing antenna design with Mg_2SnO_4 substrate.

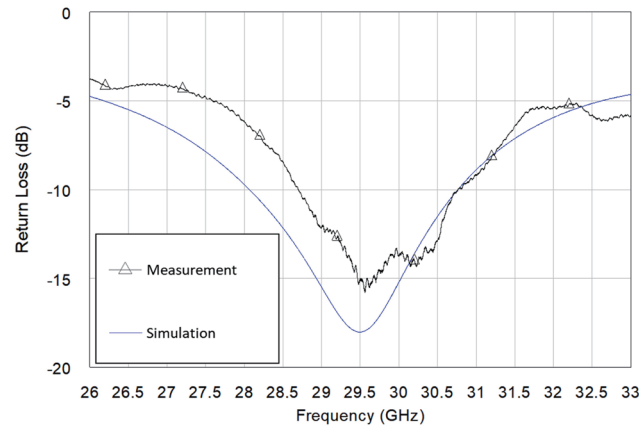


Fig. 8. (Color online) Simulation and measurement results of return loss of passive patch antenna on Mg_2SnO_4 substrate.

return loss, and bandwidth obtained by simulation were 29.494 GHz, -18.02 dB, and 5204 MHz, respectively. The measured resonant frequency, return loss, and bandwidth were 29.560 GHz, -15.79 dB, and 3635 MHz, respectively. The simulation and measurement results were in good agreement.

The temperature coefficient of the resonant frequency (τ_f), temperature coefficient of the dielectric constant (τ_K), and coefficient of linear thermal expansion (α) are related by the following formula:

$$\tau_f = -\frac{1}{2}\tau_K - \alpha, \quad (1)$$

where α is about 10 ppm/ $^{\circ}\text{C}$ for most ceramic materials.⁽²⁹⁾ From Eq. (2), the theoretical temperature coefficient of the dielectric constant was calculated to be 108 ppm/ $^{\circ}\text{C}$. Every 100 $^{\circ}\text{C}$ increase in temperature will increase the dielectric constant by 0.0429. When the operation temperature was increased from 25 to 225 $^{\circ}\text{C}$, the dielectric constant increased from 3.970 to 4.056. The calculated dielectric constant and the resonant frequency of the passive patch antenna temperature sensor obtained by simulation for different operating temperatures are summarized in Table 1.

Figure 9 shows the measurement insertion loss of the passive patch antenna temperature sensor as a function of temperature. As shown in Table 2, the resonant frequency decreased from 30.6210 to 30.3790 GHz when the operating temperature was increased from 25 to 225 $^{\circ}\text{C}$. The resonant frequency decreased as the operating temperature increased. This agreed with the temperature characteristic for a patch antenna temperature sensor composed of Mg_2SnO_4 . The resonant frequency shifted up or down with the operating temperature, as expected. Therefore, the patch antenna composed of Mg_2SnO_4 can be used as a temperature sensor. The insertion loss increased from 11.73 to 11.92 dB as the operating temperature was increased from 25 to 225 $^{\circ}\text{C}$, because the dielectric loss for the ceramic substrate increases with the temperature. At

Table 1

Calculated dielectric constant and simulation resonant frequency of passive patch antenna temperature sensor at different operating temperatures.

Temperature (°C)	Dielectric constant	Resonant frequency (GHz)
25	3.970	30.6094
50	3.981	30.5881
75	3.991	30.5631
100	4.002	30.5413
125	4.013	30.5050
150	4.024	30.4694
175	4.034	30.4356
200	4.045	30.4163
225	4.056	30.3869

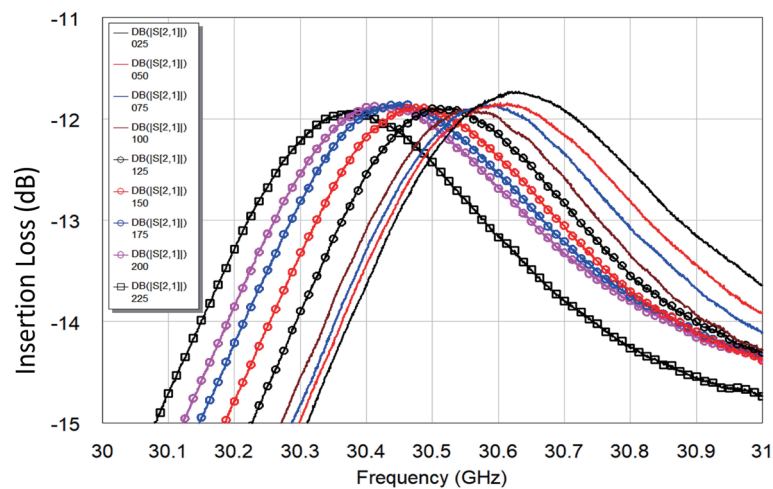


Fig. 9. (Color online) Measurement insertion loss of passive patch antenna temperature sensor.

Table 2

Measured resonant frequency, insertion loss, and bandwidth of passive patch antenna temperature sensor at different operating temperatures.

Temperature (°C)	Measured resonant frequency (GHz)	Bandwidth (MHz)	Bandwidth (%)
25	30.621	1530	5.00
50	30.603	1690	5.52
75	30.579	1820	5.95
100	30.547	2100	6.88
125	30.510	2170	7.11
150	30.471	2220	7.29
175	30.453	2390	7.85
200	30.413	2430	7.99
225	30.379	2450	8.07

temperatures of 25 and 225 °C, the 3 dB bandwidths were 1530 and 2450 MHz, respectively, corresponding to 3 dB bandwidths of 5.00 and 8.07%, respectively. The 3 dB bandwidth was correlated with the loss tangent for the ceramic substrate. The narrower the bandwidth, the greater the resolution of the antenna temperature sensor.

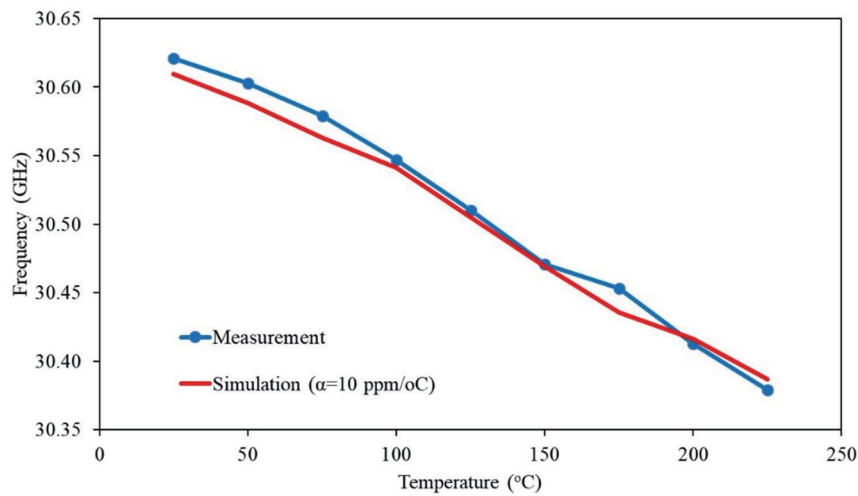


Fig. 10. (Color online) Resonant frequencies of passive patch antenna temperature sensor obtained by simulation and measurement.

Figure 10 shows the resonant frequencies of the passive patch antenna temperature sensor at different temperatures obtained by simulation and measurement. The simulation and measurement results were very similar. As the temperature increased from 25 to 225 °C, the simulation resonant frequency decreased from 30.6094 to 30.3869 GHz, corresponding to sensitivity and linearity of -1.113 MHz/°C and 0.05%, respectively. The measured resonant frequency decreased from 30.6210 to 30.3790 GHz, corresponding to sensitivity and linearity of -1.210 MHz/°C and 0.06%, respectively. The resonant frequencies of the passive patch antenna temperature sensor obtained by measurement and simulation are summarized in Table 2. The passive patch antenna temperature sensor using a Mg_2SnO_4 substrate had a low loss tangent and high sensitivity. Passive patch antenna temperature sensors using a Mg_2SnO_4 substrate are more suitable than commercial substrates for applications in harsh environments.^(16–18) Furthermore, the investigated mm-wave-based patch antenna temperature sensor had a smaller size than the sensing antenna resonating at 5.862 GHz in Ref. 6. Moreover, the investigated passive patch antenna temperature sensor adopted the orthogonal polarization method to measure the signal, which makes subsequent time gating and data processing unnecessary.^(18,20) These features mean that the investigated passive patch antenna temperature sensor is eminently suitable for the construction of a high-temperature sensor.

4. Conclusions

In this study we determined the millimeter dielectric properties of Mg_2SnO_4 ceramic and developed a passive patch antenna temperature sensor. The sensing and transceiver antennas employed Mg_2SnO_4 and RO3003 substrates, respectively, and were subjected to a laser engraving process. In experiments, the passive patch antenna temperature sensor exhibited a sensitivity of -1.210 MHz/°C, a linearity of 0.06%, and a maximum operating temperature of 225 °C. A passive patch antenna temperature sensor with a high-quality-factor ceramic substrate

is eminently suitable for applications in harsh industrial environments. The sensor not only has high sensitivity and excellent linearity but can also perform measurements in a short time at a low cost.

Acknowledgments

The authors would like to thank the National Science Council in Taiwan for financially supporting this research under Contract No. MOST 110-2221-E-262-004-.

References

- 1 J. A. Zhang, B. R. Lan, Y. J. Lin, T. J. Luo, C. H. Lu, R. H. Liu, and B. K. Chen: *J. Taiwan Energy* **1** (2014) 259. https://km.twenergy.org.tw/Publication/thesis_more?id=31
- 2 K. Nguessan, E. Jouseau, G. Rostaing, and F. Francois: 2006 IEEE Int. Conf. Industrial Technology (IEEE, 2006) 506.
- 3 P. R. N. Childs, J. R. Greenwood, and C. A. Long: *Rev. Sci. Instrum.* **71** (2000) 2959. <https://aip.scitation.org/doi/10.1063/1.1305516>
- 4 S. Y. Kim, J. D. Kim, Y. S. Kim, H. J. Song, and C. Y. Park: *Sens. Mater.* **28** (2016) 661. <https://myukk.org/SM2017/article.php?ss=1320>
- 5 B. Lee: *Opt. Fiber Technol.* **9** (2003) 57. <https://www.sciencedirect.com/science/article/abs/pii/S1068520002005278>
- 6 J. W. Sanders, J. Yao, and H. Huang: *IEEE Sens. J.* **15** (2015) 5312. <https://ieeexplore.ieee.org/document/7113781>
- 7 C. Mandel, B. Kubina, M. Schübler, and R. Jakoby: *Ann. Telecommun.* **68** (2013) 385. <https://link.springer.com/article/10.1007/s12243-013-0372-9>
- 8 B. Kubina, C. Mandel, M. Schübler, M. Sazegar, and R. Jakoby: *Proc. 42nd European Microwave Conf. (IEEE, 2012)* 61.
- 9 R. Melik, E. Unal, N. K. Perkgoz, B. Santoni, D. Kamstock, C. Puttlitz, and H. V. Demir: *IEEE J. Sel. Top. Quantum Electron.* **16** (2010) 450. <https://ieeexplore.ieee.org/document/5361333>
- 10 T. T. Thai, H. Aubert, P. Pons, R. Plana, M. M. Tentzeris, and G. R. DeJean: *IEEE Sensors Conf. (IEEE, 2011)* 211.
- 11 K. H. Hoffmann: *Functional Micro and Nano Systems* (Springer, Bonn, 2003) 4nd ed., Chap. 8.
- 12 D. W. Greve, T. L. Chin, P. Zheng, P. Ohodnicki, J. Baltrus, and I. J. Oppenheim: *Sensors* **13** (2013) 6910. <https://www.mdpi.com/1424-8220/13/6/6910>
- 13 X. Ye, Q. Wang, L. Fang, X. Wang, and B. Liang: *IEEE Sensors 2010 Conf. (IEEE, 2010)* 585.
- 14 S. Scott and D. Peroulis: *IEEE MTT-S Int. Microwave Symp. Digest (IEEE, 2009)* 1161.
- 15 J. M. Boccard, T. Aftab, J. Hoppe, A. Yousaf, R. Hutter, and L. M. Reindl: *IEEE Sens. J.* **16** (2016) 715. <https://ieeexplore.ieee.org/document/7293087>
- 16 H. Jiang, J. Sanders, J. Yao, and H. Huang: *Nondestructive Characterization for Composite Materials, Aerospace Engineering, Civil Infrastructure, and Homeland Security 2014 (SPIE, 2014)* 90631P.
- 17 J. W. Sanders, J. Yao, and H. Huang: *IEEE Sens. J.* **15** (2015) 5312. <https://ieeexplore.ieee.org/document/7113781>
- 18 J. Yao, F. M. Tchafa, A. Jain, S. Tjuatja, and H. Huang: *IEEE Sens. J.* **16** (2016) 7053. <https://ieeexplore.ieee.org/document/7529076>
- 19 H. Kairm, D. Delfin, M. A. Shuvo, L. A. Chavez, C. R. Garcia, J. H. Barton, S. M. Gaytan, M. A. Cadena, R. C. Rumpf, R. B. Wicker, Y. Lin, and C. Ahsan: *IEEE Sens. J.* **15** (2015) 1445. <https://ieeexplore.ieee.org/abstract/document/6924738>
- 20 Y. C. Chen, and Y. X. Du: *J. Mater. Sci.: Mater. Electron.* **29** (2018) 18432. <https://doi.org/10.1007/s10854-018-9958-3>
- 21 C. G. Shih, W. M. Li, M. M. Lin, C. Y. Hsiao, and K. T. Hung: *J. Alloys Compd.* **485** (2009) 408. <https://www.sciencedirect.com/science/article/abs/pii/S0925838809010962?via%3Dihub>
- 22 Y. C. Chen, C. F. Su, M. Z. Weng, H. M. You, and K. C. Chang: *J. Mater. Sci.: Mater. Electron.* **25** (2014) 2120. <https://www.springerprofessional.de/en/improvement-microwave-dielectric-properties-of-zn2sno4-ceramics-/3553154>
- 23 Y. C. Chen, Y. N. Wang, and C. H. Hsu: *J. Alloys Compd.* **509** (2011) 9650. <https://www.sciencedirect.com/science/article/abs/pii/S0925838811015611>

- 24 Y. C. Chen and C. H. Li: Ceram. Int. **42** (2016) 9749. <https://www.sciencedirect.com/science/article/pii/S0272884216301948?via%3Dihub>
- 25 B. W. Hakki and P. D. Coleman: IEEE Trans. Microwave Theory Tech. **8** (1960) 402. <https://ieeexplore.ieee.org/stamp/stamp.jsp?arnumber=1124749>
- 26 N. K. Das, S. M. Voda, and D. M. Pozar: IEEE Trans. Microwave Theory Tech. **35** (1987) 636. <https://ieeexplore.ieee.org/document/1133722/>
- 27 Y. Tohdo, K. Kakimoto, H. Ohsato, H. Yamada, and T. Okawa: J. Eur. Ceram. Soc. **26** (2006) 2039. <https://www.sciencedirect.com/science/article/pii/S0955221905008472?via%3Dihub>
- 28 A. A. Ward: Dielectric Materials for Advanced Applications (National Research Center, Egypt, 2015) Chap. 2. <https://www.researchgate.net/publication/304101071>
- 29 M. T. Sebastian: Dielectric Materials for Wireless Communication (Elsevier, Oxford, 2008) Chap. 2. <https://www.sciencedirect.com/book/9780080453309/dielectric-materials-for-wireless-communication>

About the Authors

Ying-Ting Liao received his B.S. and M.S. degrees in electrical engineering from Lunghwa University of Science and Technology, Taoyuan, Taiwan, in 2017 and 2020, respectively. He is currently a Ph.D. student in the Department of Electrical Engineering, National Taiwan University of Science and Technology, Taipei, Taiwan. His research interests are in microwave engineering, microwave ceramics, and embedded system applications. (ce034@gm.lhu.edu.tw)

Yih-Chien Chen received his B.S., M.S., and Ph.D. degrees in electrical engineering from National Cheng Kung University, Tainan, Taiwan, in 1994, 1996, and 2000, respectively. He is currently a Distinguished Professor in the Department of Electrical Engineering, Lunghwa University of Science and Technology, Taoyuan, Taiwan. His research interests are in microwave engineering, microwave ceramics, and sensors. (ee049@mail.lhu.edu.tw)

Cheng-Chien Kuo received his B.S., M.S., and Ph.D. degrees in electrical engineering from National Taiwan University of Science and Technology, Taipei, Taiwan, in 1991, 1993, and 1998, respectively. He is currently a professor in the Department of Electrical Engineering, National Taiwan University of Science and Technology. His research interests are in power electronics, energy monitoring, and embedded system applications. (cckuo@mail.ntust.edu.tw)